Luminescence from bismuth-germanate glasses and its manipulation through oxidants

A. Winterstein,[1] S. Manning,[2] H. Ebendorff-Heidepriem,[2] and L. Wondraczek[1,3,*]

[1]*Department Material Science, University of Erlangen-Nuremberg, 91058 Erlangen, Germany*
[2]*Institute for Photonics & Advanced Sensing, The University of Adelaide, Adelaide, SA 5005, Australia*
[3]*Otto-Schott-Institute, University of Jena, 07745 Jena, Germany*
**lothar.wondraczek@uni-jena.de*

Abstract: We report on the luminescence properties of bismuth-germanate glasses in which the speciation of bismuth is controlled via addition of CeO_2 as an oxidant. A glass system with the composition $(70.5\text{-}x)GeO_2$ – $24.5Bi_2O_3$ – $5WO_3$: $xCeO_2$, with x = 0...2.0, is analyzed in terms of optical properties and redox states of bismuth and cerium. We show that optical transmission and luminescence in the visible to near-infrared (NIR) spectral range can be adjusted by the ratio of bismuth and cerium. Specifically, ultra-broad NIR luminescence spanning the range of 1000 – 1600 nm can be obtained for $x \leq 0.1$. This is of particular interest for application of this type of glass in fiber-optical amplifiers where no additional dopants would be required.

OCIS codes: (160.2750) Glass and other amorphous materials; (160.2540) Fluorescent and luminescent materials; (140.4480) Optical amplifiers; (060.4510) Optical communications.

References and links

1. K. Richardson, D. Krol, and K. Hirao, "Glasses for photonic applications," Int. J. Appl. Glass Sci. **1**(1), 74–86 (2010).
2. M. Peng, C. Zollfrank, and L. Wondraczek, "Origin of broad NIR photoluminescence in bismuthate glass and Bi-doped glasses at room temperature," J. Phys. Condens. Matter **21**(28), 285106 (2009).
3. J. Lucas, "Infrared fibers," Infrared Phys. **25**(1-2), 277–281 (1985).
4. W. H. Dumbaugh and J. C. Lapp, "Heavy metal oxide glasses," J. Am. Ceram. Soc. **75**(9), 2315–2326 (1992).
5. D. L. Wood, K. Nassau, and D. L. Chadwick, "Optical properties of new oxide glasses with potential for long-wavelength optical fibers," Appl. Opt. **21**(23), 4276–4279 (1982).
6. S. S. Rojas, J. E. De Souza, M. R. B. Andreeta, and A. C. Hernandes, "Influence of ceria addition on thermal properties and local structure of bismuth germanate glasses," J. Non-Cryst. Solids **356**(52-54), 2942–2946 (2010).
7. M. Peng, N. Da, S. Krolikowski, A. Stiegelschmitt, and L. Wondraczek, "Luminescence from Bi^{2+}-activated alkali earth borophosphates for white LEDs," Opt. Express **17**(23), 21169–21178 (2009).
8. M. Peng and L. Wondraczek, "Photoluminescence of $Sr_2P_2O_7$:Bi^{2+} as a red phosphor for additive light generation," Opt. Lett. **35**(15), 2544–2546 (2010).
9. M. Peng and L. Wondraczek, "Bi^{2+}-doped strontium borates for white-light-emitting diodes," Opt. Lett. **34**(19), 2885–2887 (2009).
10. Y. Fujimoto and M. Nakatsuka, "Infrared luminescence from bismuth-doped silica glass," Jpn. J. Appl. Phys. **40**(Part 2, No. 3B), L279–L281 (2001).
11. R. Cao, M. Peng, L. Wondraczek, and J. Qiu, "Superbroad near-to-mid-infrared luminescence from Bi_5^{3+} in $Bi_5(AlCl_4)_3$," Opt. Express **20**(3), 2562–2571 (2012).
12. S. Khonthon, S. Morimoto, Y. Arai, and Y. Ohishi, "Luminescence characteristics of Te- and Bi-doped glasses and glass-ceramics," J. Ceram. Soc. Jpn. **115**(1340), 259–263 (2007).
13. V. O. Sokolov, V. G. Plotnichenko, and E. M. Dianov, "Origin of broadband near-infrared luminescence in bismuth-doped glasses," Opt. Lett. **33**(13), 1488–1490 (2008).
14. K. H. Nielsen, M. M. Smedskjaer, M. Peng, Y. Z. Yue, L. Wondraczek, communicated to J. Non-Cryst. Solids (2012).
15. W. A. Weyl, *Coloured Glasses,* 5th ed. (Sheffield: Society of Glass Technology, 1999).
16. M. Peng, B. Sprenger, M. A. Schmidt, H. G. Schwefel, and L. Wondraczek, "Broadband NIR photoluminescence from Bi-doped $Ba_2P_2O_7$ crystals: insights into the nature of NIR-emitting bismuth centers," Opt. Express **18**(12), 12852–12863 (2010).

#172414 - $15.00 USD Received 11 Jul 2012; revised 13 Aug 2012; accepted 14 Aug 2012; published 31 Aug 2012

17. X. Jiang and A. Jha, "An investigation on the dependence of photoluminescence in Bi_2O_3-doped GeO_2 glasses on controlled atmospheres during melting," Opt. Mater. **33**(1), 14–18 (2010).
18. M. Peng, Q. Zhao, J. Qiu, and L. Wondraczek, "Generation of emission centers for broadband NIR luminescence in bismuthate glass by femtosecond laser irradiation," J. Am. Ceram. Soc. **92**(2), 542–544 (2009).
19. V. Dvoyrin, V. Mashinsky, and E. Dianov, "Efficient bismuth-doped fiber lasers," IEEE J. Quantum Electron. **44**(9), 834–840 (2008).
20. K. Murata, Y. Fujimoto, T. Kanabe, H. Fujita, and M. Nakatsuka, "Bi-doped SiO_2 as a new laser material for an intense laser," Fusion Eng. Des. **44**(1-4), 437–439 (1999).
21. M. Peng, J. Qiu, D. Chen, X. Meng, and C. Zhu, "Superbroadband 1310 nm emission from bismuth and tantalum codoped germanium oxide glasses," Opt. Lett. **30**(18), 2433–2435 (2005).
22. M. Peng, N. Zhang, L. Wondraczek, J. Qiu, Z. Yang, and Q. Zhang, "Ultrabroad NIR luminescence and energy transfer in Bi and Er/Bi co-doped germanate glasses," Opt. Express **19**(21), 20799–20807 (2011).
23. M. Peng, G. Dong, L. Wondraczek, L. Zhang, N. Zhang, and J. Qiu, "Discussion on the origin of NIR emission from Bi-doped materials," J. Non-Cryst. Solids **357**(11-13), 2241–2245 (2011).
24. M. Peng and L. Wondraczek, "Bismuth-doped oxide glasses as potential solar spectral converters and concentrators," J. Mater. Chem. **19**(5), 627–630 (2009).
25. X. G. Meng, J. R. Qiu, M. Y. Peng, D. P. Chen, Q. Z. Zhao, X. W. Jiang, and C. S. Zhu, "Infrared broadband emission of bismuth-doped barium-aluminum-borate glasses," Opt. Express **13**(5), 1635–1642 (2005).
26. S. Khonthon, S. Murimoto, Y. Arai, and Y. Ohishi, "Near infrared luminescence from Bi-doped soda lime silicate glasses," Suranaree J. Sci. Technol. **14**, 141–146 (2007).
27. M. A. Hughes, T. Akada, T. Suzuki, Y. Ohishi, and D. W. Hewak, "Ultrabroad emission from a bismuth doped chalcogenide glass," Opt. Express **17**(22), 19345–19355 (2009).
28. W. Wang, Q. Yan, J. Ren, G. Chen, N. Da, and L. Wondraczek, "Ultrabroad near-infrared photoluminescence from Bi/Dy/Tm co-doped chalcohalide glasses," Phys. Chem. Glasses: Eur. J. Glass Sci. Technol. B **52**(6), 221–224 (2011).
29. J. D. Barrie, L. A. Momoda, B. Dunn, D. Gourier, G. Aka, and D. Vivien, "ESR and optical spectroscopy of Ce3+: β″-alumina," J. Solid State Chem. **86**(1), 94–100 (1990).
30. T. Inoue, T. Honma, V. Dimitrov, and T. Komatsu, "Approach to thermal properties and electronic polarizability from average single bond strength in ZnO-Bi_2O_3-B_2O_3 glasses," J. Solid State Chem. **183**(12), 3078–3085 (2010).
31. V. Dimitrov and T. Komatsu, "Average single bond strength and optical basicity of Na_2O-GeO_2 glasses," J. Ceram. Soc. Jpn. **117**(1370), 1105–1111 (2009).
32. V. Dimitrov and T. Komatsu, "An interpretation of optical properties of oxides and oxide glasses in terms of the electronic ion polarizability and average single bond strength," J. Univ. Chem. Technol. Metall. **45**, 219–250 (2010).
33. H. Bach, F. Baucke, and D. Krause, *Electrochemistry of Glasses and Glass Melts, Including Glass Electrodes* (Springer, 2001), p. 293.
34. G. Chen, S. Baccaro, A. Cecilia, Y. Du, M. Montecchi, J. Nie, S. Wang, and Y. Zhang, "Ultraviolet and visible transmission spectra of heavy germanate glasses containing Sn^{2+} and Ce^{3+}," J. Non-Cryst. Solids **326-327**, 343–347 (2003).
35. N. Haage, K. H. Hellwege, J. Jäger, and G. Schaack, "Absorptionsspektrum des Ce^{3+}-ions und Schwingungsspektrum im $CeCl_3 \cdot 7H_2O$ und $CeCl_3 \cdot 7D_2O$," Phys. Kondens. Mater. **10**, 144–151 (1969).
36. S. Zhou, N. Jiang, B. Zhu, H. Yang, S. Ye, G. Lakshminarayana, J. Hao, and J. Qiu, "Multifunctional bismuth-doped nanoporous silica glass: from blue-green, orange, red, and white light sources to ultra-broadband infrared amplifiers," Adv. Funct. Mater. **18**(9), 1407–1413 (2008).
37. H. You, T. Hayakawa, and M. Nogami, "Upconversion luminescence of Al_2O_3–SiO_2:Ce^{3+} glass by femtosecond laser irradiation," Appl. Phys. Lett. **85**(16), 3432–3434 (2004).
38. O. Shestakov, R. Breidohr, H. Demes, K. D. Setzer, and E. H. Fink, "Electronic states and spectra of BiO," J. Mol. Spectrosc. **190**(1), 28–77 (1998).
39. L. Su, J. Yu, P. Zhou, H. Li, L. Zheng, Y. Yang, F. Wu, H. G. Xia, and J. Xu, "Broadband near-infrared luminescence in γ-irradiated Bi-doped α-BaB_2O_4 single crystals," Opt. Lett. **34**(16), 2504–2506 (2009).

1. Introduction

For applications in the near-infrared spectral range (NIR), other glass systems besides silica have demonstrated growing interest [1,2]. Germanate glasses exhibit several advantageous properties such as high chemical, mechanical and thermal stability [1]. They offer a variety of material properties for numerous applications, ranging from low-loss optical fiber for telecommunication with a wider transmission window to photonic crystal fibres, sensors and amplifiers for the NIR [1,3]. With addition of heavy metal oxides such as bismuth- and lead-oxides, the transparency of germanate glasses can be extended into the mid-infrared up to 6 μm [4,5]. Here, Bismuth(III)oxide has the advantage of intoxicity in comparison to lead oxide. Incorporated in glasses, Bi_2O_3 can be either network modifier or network former, depending on other glass components and concentration, and can therefore further contribute

#172414 - $15.00 USD Received 11 Jul 2012; revised 13 Aug 2012; accepted 14 Aug 2012; published 31 Aug 2012

to chemical, mechanical and thermal stability. In the presence of conventional glass formers such as Ge^{4+}, Si^{4+}, B^{3+} and P^{5+}, Bi^{3+} coordinates mostly in BiO_3-pyramidal and BiO_6-octahedral units which, due to the fact that Bi^{3+} ions are highly polarizable, form a secondary network structure [6]. When bismuth is present in other forms than the 3^+-state, it is typically expected to act as a network modifier which will be incorporated into the glass lattice by breaking-up the network structure and, therefore, reduce the glass transition temperature.

The redox state in which bismuth is present in an oxide matrix is highly sensitive to the (structural) environment, the basicity of the matrix components and various processing parameters. In principle, a large number of species is possible, ranging from Bi^{3+} as the predominant species in common applications to lower redox states such as Bi^+ and Bi^{2+} [2,7–9], or higher oxidized species such as Bi^{5+} [10]. In addition, various subvalent species and ion clusters [11–13], Bi^0 or metallic bismuth particles have been reported. The question as to which species are dominant in a given material has significant consequences for the material's optical properties, which makes it crucial to delicately control the redox conditions [14]. For example, decreasing the redox state of bismuth towards the formation of metallic nanoparticles has been known as an easy method to tune glass color from yellow to reddish tints to deep black [15]. To prevent the formation of lower-valence bismuth states during glass fabrication, several methods have been explored, such as calcination of the precursors, different annealing temperatures, shorter melting times and the use of different crucible materials [2,16,17]. Another possibility to prevent reduction is through oxidants, MeO_x, which provide oxygen to the glass system while the cation is embedded in the network. The use of an oxidant provides a major advantage in comparison to the other methods as it needs no specific and time consuming process variation or secondary batch treatment procedures. The oxidant used in this work was CeO_2 [6,18].

By adding the ceria(IV) oxide to bismuth-germanate glasses, the bismuth ion keeps the redox state of the raw material Bi_2O_3, which is Bi^{3+}. Only small molar percentages are needed to avoid the darkening of the glass. Particularly for the fabrication of highly transparent bismuth-germanate optical fiber, it is important to understand the structural influence of cerium species and the quantitative effect of the decolorization of bismuth-germanate glasses.

However, also the lower redox states of bismuth are of some interest as they may show unique luminescence behavior in the visible and NIR range. If this could be further exploited, it could have significant implications for fiber lasers and optical amplifiers [19]. For example, after the first observation of ultrabroad NIR luminescence in Bi-doped silica glass by Murata et al. [20], NIR emission has been demonstrated in many glass systems, including several germanate glasses [17,21,22]. Despite the obvious interest for optical fiber devices, there is still no consensus regarding the origin of the NIR-luminescence [23], although most authors attribute it to lower redox states of bismuth. From a technical point of view, the darkening of the glass, which is associated with bismuth being in low oxidation states, is a disadvantage for transmittance in the visible and needs to be chosen in accordance to the application. Ideally, the redox state would be manipulated so that the required optical transmission is maintained, but also advantageous luminescence behavior is achieved.

The wavelength and the intensity of the emitted light depend on the local structure surrounding the bismuth ions as a result of ligand field strength. That is, coordination of the cations, distortions in the structural units around the cation and (phonon-assisted) energy transfer may influence the excitation and emission wavelengths of the active ion. Luminescence from Bi^{3+} typically occurs in the UV-blue spectral range, Bi^{2+} emits in the red-NIR. Both species can be excited in the UV to blue, depending on the glass system. Excitation wavelengths of 250 – 450 nm are commonly used [8,9]. Ultrabroad NIR emission follows a rather complex excitation scheme where various excitation bands occur throughout the UV-NIR spectral range [2,21,24]. As already noted, it is not exactly clear which redox state causes this emission, but it is assumed that the NIR luminescence originates from lower redox states such as Bi^+ or ion clusters [2]. For example, Meng et al. showed that with increasing basicity

#172414 - $15.00 USD Received 11 Jul 2012; revised 13 Aug 2012; accepted 14 Aug 2012; published 31 Aug 2012

of the glass, the NIR emission disappeared [25]. As a higher basicity favors a higher valence state of bismuth, it is likely that the emission in the NIR occurs from lower redox states of bismuth. It has also been shown that the use of reducing agents could improve the emission intensity as long as no metallic particles are generated [2,14]. As an empirical rule, the optimal excitation wavelength for the species Bi^x (with x = 0; 1 + ; 2 +) is typically found in the range of 500 – 800 nm, whereas the emission band lies usually in the range of 1000 – 1700 nm [10–26] (however, also mid-infrared emission has been reported for, e.g., chalcogenide matrices) [27,28]. These spectral ranges demonstrate great interest for a variety of communication, amplification and sensing applications.

In this paper, we investigate the influence of cerium(IV)oxide on the optical properties of bismuth-germanate glasses and the change of the redox state of Bi. Glasses with varying cerium concentration were analyzed to gain insight into the trade-off between optical transparency (bismuth oxidation) and NIR luminescence (bismuth reduction).

2. Experimental

2.1 Sample preparation

Glass samples of the composition (mol.%) $(70.5\text{-}x)GeO_2 – 24.5Bi_2O_3 – 5WO_3$: $xCeO_2$, with x = 0; 0.1; 0.2; 0.5; 1; 2 were produced from batches of oxide powders. Anhydrous GeO_2, Bi_2O_3, WO_3 and CeO_2 with a purity of 99.99 + % were weighed (± 5 µg) and transferred into alumina crucibles. In a first step, calcination was done in a conventional muffle furnace (Nabertherm; HT16) at 500 – 700 °C for 1h. Afterwards, the same furnace was heated at a rate of 3 K/min to a temperature of 1200 °C and held at this temperature for 40 min. The obtained glass melt was then poured into preheated (450 °C) brass moulds. Finally, glass slabs were annealed at 490 °C for 1 h, using another muffle furnace (Linn, LM 31227) and cooled to room temperature at a rate of approximately 2 K/min. Samples were subsequently cut into thin disks (with a thickness of 2.45 - 2.7 mm) and mechanically polished in several steps to optical quality with a final polishing slurry grain size of 5 µm.

2.2 Spectroscopic characterization

To characterize the redox state of the as-melted glasses, the presence of Ce^{3+} was analyzed by electron spin resonance spectroscopy (EPR) and optical spectroscopy. EPR was conducted at a frequency of 9.8 GHz (Bruker, ESP 300E) on powder samples. Optical absorption data was collected over the spectral range of 200 nm to 2500 nm in a UV-NIR spectrophotometer (Perkin Elmer, Lambda 950), equipped with a 150 mm integration sphere. Fourier-transform infrared (FTIR) spectroscopic measurements (Nicolet, Impact 420) were performed in transmission mode in the region of 2500 nm – 10000 nm. All FTIR spectra were normalized and corrected for background signals, Fresnel reflection and surface imperfection prior to calculation of the absorption coefficient. Static and dynamic fluorescence spectra were recorded on a high-resolution spectrofluorometer (Horiba Jobin Yvon, Flourolog 3-22), equipped with double monochromators in excitation and emission. A static Xe lamp (450 W) and a Xe flashlamp (75 W) were used as excitation sources for static and dynamic analyses, respectively. The slit size of both the excitation monochromator and the emission monochromator was 5 nm for all measurements. The NIR-signal was recorded with a thermoelectrically cooled InP/InGaAs-photomultiplier tube (NIR-PMT, Hamamatsu H10330A-75), operating in the spectral range of 900 - 1700 nm.

3. Results and discussion

3.1 Optical absorption

Ceria(IV) doping has a pronounced effect on the color of the examined glass system (Fig. 1(a)). In a first inspection, all glasses show high optical quality with no visible striae, bubbles, inclusions or cracks. With increasing the content of CeO_2, the visual coloration first decreases

#172414 - $15.00 USD Received 11 Jul 2012; revised 13 Aug 2012; accepted 14 Aug 2012; published 31 Aug 2012

from black to deep red to light yellow at $x = 0.2$. For $x > 0.2$, the tint re-intensifies to deep orange and brownish red at $x = 2.0$. This phenomenology it attributed to the overlapping effects of bismuth oxidation ($x \leq 0.2$), increasing absorption associated to Ce^{3+} species ($x \geq 0.2$) and potential secondary, more complex redox relations which lead to the formation of further coloring bismuth species. Ce^{3+} is formed through reduction of Ce^{4+} in the $Bi^{(3-i)+}/Ce^{4+}$ redox pair ($i = 1...3$). While Ce^{4+} is EPR inactive, the occurrence of Ce^{3+} can be detected using EPR spectroscopy. Ce^{3+}-related defect centers shows weak bands at around 1400 G (g ~4.1) and 3000 G (g ~2.6) [29]. Qualitative EPR analyses have therefore been employed to explore the change in the cerium redox state in the glasses with different cerium concentration. No Ce^{3+}-related signals could be detected in the CeO_2-free glass, whereas both mentioned bands were found to increase significantly with increasing CeO_2 doping. This demonstrates that a significant part of the doped Ce^{4+} species is reduced to Ce^{3+} during glass melting. Optical basicity and redox activities are not reported for the glass system of this study. Using estimates for the partial molar optical basicity of GeO_2, BiO_2, WO_3 and CeO_2, Λ_{GeO2} ~0.7, Λ_{Bi2O3} ~1.19, Λ_{WO3} ~1.04 and Λ_{CeO2} ~1.01 [30–32], we derive a relatively high value for the optical basicity of Λ ~0.83 for the employed series of glasses. In a further approximation, we assume that the absolute amount of bismuth is large compared to the absolute amount of cerium, and that the redox pair of $Bi^{(3-i)+}/Ce^{4+}$ behaves similar to the pair of Tl^{+}/Ce^{4+}. For the latter, redox ratios have been reported for silicate matrices, $\log[Tl^{+}/Tl^{3+}]$ ~13 - 20Λ and $\log[Ce^{3+}/Ce^{4+}]$ ~5.4 - 8.3Λ at 1400 °C [33].

Formally, we further assume the symbolic reaction

$$2Ce^{4+} + Bi^{+} \leftrightarrow 2Ce^{3+} + Bi^{3+}, \tag{1}$$

which governs oxidation of Bi^{+} species and formation of Ce^{3+}. For this reaction, the equilibrium constant is given by Eq. (2)

$$\log K_c = 2\log\frac{[Ce^{3+}]}{[Ce^{4+}]} - \log\frac{[Bi^{+}]}{[Bi^{3+}]}. \tag{2}$$

With above assumptions, it is $\log K_c = 3.4\Lambda$ - 2.2 ~4, which means that the equilibrium of the reaction shown in Eq. (1) lies on the side of the products and more than 70% of the Ce^{4+} ions have been reduced to Ce^{3+}.

Optical absorption spectra of the glasses with varying CeO_2 dopant concentration are shown in Fig. 1(b). In the absence of CeO_2 ($x = 0$), a strong absorption band occurs in the spectral range of 500 – 600 nm with peak intensity of 10.7 cm^{-1}. This band is assigned to lower valency Bi-species [2]. With increasing CeO_2 concentration, the intensity of this band decreases, i.e. to 2.3 cm^{-1} at $x = 0.1$, and cannot be detected anymore at $x = 0.2$ or higher. For larger CeO_2 concentrations, the absorption edge shifts to longer wavelengths, i.e. the optical Band gap decreases from ~2.5 eV to ~1.5 eV (determined by the Tauc method). The sample with $x = 0.2$ exhibits the largest Band gap. This reflects that in sample $x = 0.0$ and $x = 0.1$ the absorption of Bi^{2+} and lower valence states of bismuth is dominant. On the other hand, at larger CeO_2 content, absorption is determined by the presence of cerium and associated charge transfer reactions which lead to the red-shift of the lower absorption edge and, in particular, 4f–5d transitions in Ce^{3+} ions [34].

#172414 - $15.00 USD Received 11 Jul 2012; revised 13 Aug 2012; accepted 14 Aug 2012; published 31 Aug 2012

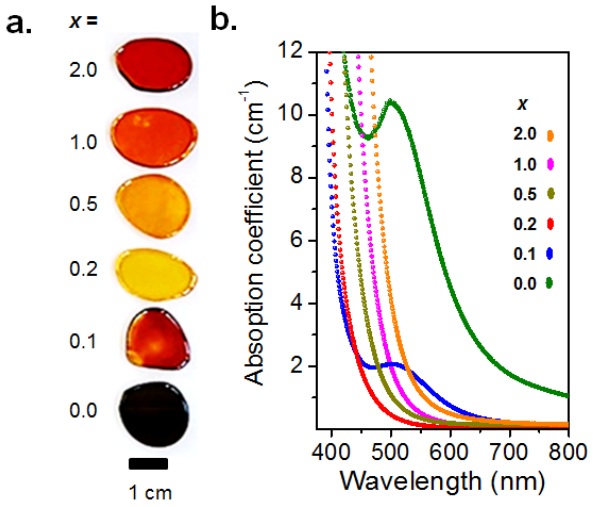

Fig. 1. Photograph of (mol%) (70.5-x)GeO_2 – 24.5Bi_2O_3 – 5WO_3: $x$$CeO_2$ glass samples for varying x (a) and corresponding optical absorption spectra (b). The photograph was taken under ambient illumination.

Figure 2(a) represents FTIR spectra of the glass samples with x = 0; 0.1; 0.2; 0.5; 1; 2. All spectra comprise a strong absorption band related to hydroxyl groups (OH^-, ~2.8-3.5 µm) and at least three further bands. The latter are readily assigned to transitions from the ground state of Ce^{3+} to the Stark levels of $^2F_{7/2}$ [35]. Of the four possible bands, three can be detected unambiguously at ~3.8, 4.2 and 4.65 µm. The fourth is superimposed by the OH^--background absorption and becomes visible only after background subtraction (see inset of Fig. 2(b)). The evolution of the peaks with increasing CeO_2-doping is in very good agreement with the expectation of an increasing amount of Ce^{3+}. For a quantitative evaluation, the x = 0 - spectrum was subtracted from each individual spectrum, assuming that OH^- and further background absorption (including absorption from eventual bismuth species) is not affected by the nominal CeO_2 - content in the considered wavelength regime (inset of Fig. 2(b)). Spectra were then integrated over the spectral range of 2.5-5.2 µm. As shown in Fig. 2(b), the obtained band area follows well a linear dependence. At constant sample thickness and constant extinction coefficient, this means that the amount of Ce^{3+} increases linearly with increasing absolute CeO_2 content. The latter is taken as a sign that within the considered range of dopant concentrations, there is no saturation or concentration-dependence of the redox reaction symbolized in Eq. (1).

The absorption by Ce^{3+} is relatively high, up to 2.6 cm^{-1} at ~4.65 µm. This needs to be considered in potential applications, as the absorption bands of Ce^{3+} lie within the intrinsic transmission window of the glass (i.e. at wavelengths shorter than the edge at 5.5 µm). OH^--related absorption can be controlled via the water content of the glass, i.e. by employing dry raw materials and adjusting process conditions.

#172414 - $15.00 USD Received 11 Jul 2012; revised 13 Aug 2012; accepted 14 Aug 2012; published 31 Aug 2012

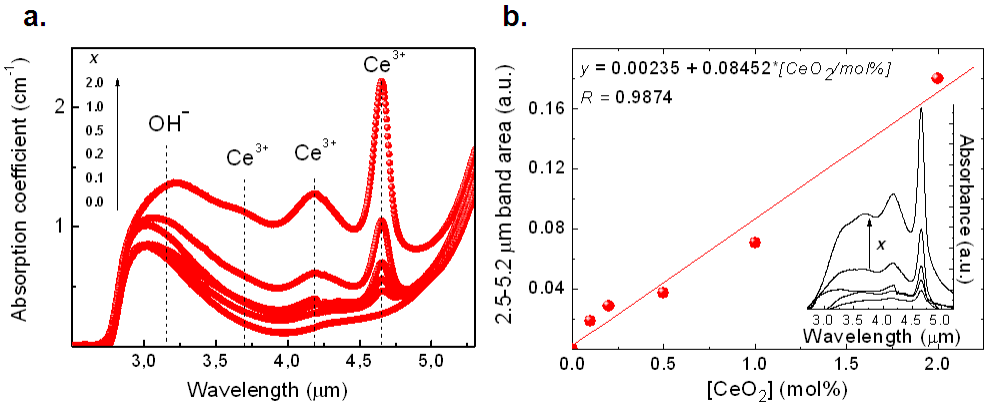

Fig. 2. FTIR absorption spectra of (mol.%) (70.5-x)GeO_2 – 24.5Bi_2O_3 – 5WO_3: $x$$CeO_2$ glass samples for varying x (a), and integrated area of the 2.5 - 5.2 μm absorption band, corrected by the absorption spectrum of the undoped sample (b). Labels in (a) indicate absorption bands of Ce^{3+} and OH^- groups. The inset of (b) shows the spectra after subtraction of the absorption spectrum of the undoped sample, assuming that residual absorption originates solely from Ce^{3+}.

3.2 Photoluminescence

Bismuth and its lower valence states, such as Bi^{2+} and Bi^+ show luminescence in the visible and NIR spectral ranges [7–28,36]. In Fig. 3, luminescence spectra of the glasses are shown as a function of CeO_2 content. Using an excitation wavelength of 368 nm, a broad emission band occurs around 650 nm (orange-red, Fig. 3(a)). This band is assigned to the transition of $^2P_{3/2}(1) \rightarrow {}^2P_{1/2}$ in Bi^{2+}, following non-radiative decay of $^2P_{3/2}(2)$ to $^2P_{3/2}(1)$ [8,9]. The signal of Ce^{3+} can be neglected as it shows emission at smaller wavelengths, i.e. 300 – 500 nm [37], this also lies in the absorption edge of these glasses and does not overlap with the emission of Bi^{2+} in the visible. The intensity of this band exhibits a maximum at $x = 0.1$, assumedly as a consequence of incomplete oxidation of $Bi^{(2-i)+}$ to Bi^{2+}. With further increasing CeO_2-content, the amount of Bi^{2+} species is reduced by oxidation to Bi^{3+}, leading to a continuous decrease in the intensity of the 650 nm emission band. Additionally, intrinsic quenching occurs due to overlaying absorption by Ce^{3+} (Fig. 1) in the same spectral range. Above an absolute CeO_2 content of 0.5 mol%, the intensity of VIS luminescence reduces drastically. This picture is confirmed by the evolution of NIR luminescence with CeO_2 content (Fig. 3(b)). For $x \leq 0.1$, a broad NIR luminescence band occurs over the spectral range of 1000 - 1600 nm (note that at wavelengths > 1600 nm, the sensitivity of the employed PMT detector drops sharply). As noted before, the origin of this NIR emission band remains disputed. For the present case and considering the shape of the spectrum, we may assume that NIR luminescence originates from more than one redox state of bismuth. That is, for Bi^{2+}, NIR emission at ~950 nm may result from electronic excitation of to the state of H, followed by non-radiative relaxation to X_2 and radiative decay to the ground state of $^2P_{1/2}$. The energy levels and their position concerning level I and X_2 have been taken from [38]. For Bi^+, the electrons can be excited from $^3P_0$ to $^3P_2$ (or $^1S_0$), relax to $^3P_1$ and decay radiatively to the ground level. These transitions are shown schematically in the energy level Fig. 4. The intensity of the NIR band decreases already in the presence of a small amount of CeO_2, i.e. for $x = 0.1$, and vanishes completely for $x > 0.1$, indicating that practically all species of bismuth with valence < 2 + have been oxidized to higher valence, and that also Bi^{2+} species are gradually erased. The presence of metallic Bi nanoparticles has been ruled-out for the present case by analysis through transmission electron microscopy and X-ray diffraction.

#172414 - $15.00 USD Received 11 Jul 2012; revised 13 Aug 2012; accepted 14 Aug 2012; published 31 Aug 2012

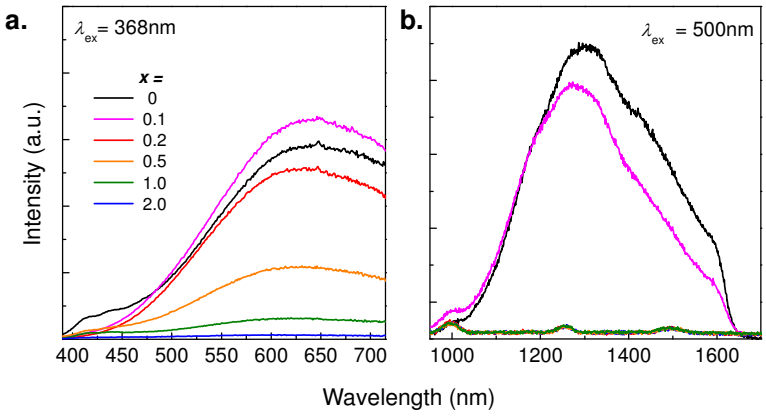

Fig. 3. Luminescence spectra of (mol.%) (70.5-x)GeO_2 – 24.5Bi_2O_3 – 5WO_3: $x$$CeO_2$ glass samples for varying x at an excitation wavelength of 368 nm (a) and 500 nm (b), respectively.

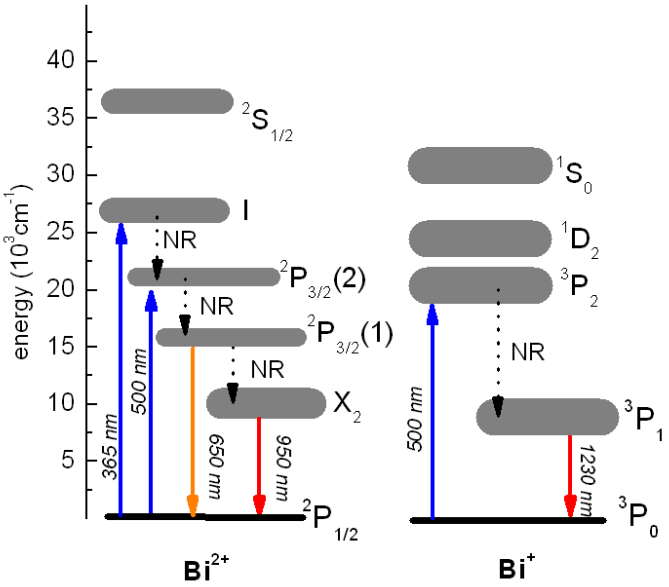

Fig. 4. Simplified energy level diagram for Bi^{2+} (left) and Bi^+ (right). The arrows indicate potential excitation and relaxation paths.

Exemplary emission decay curves for VIS and NIR luminescence, respectively, are given in Fig. 5. Decay clearly does not follow a single exponential function. This indicates that for both cases (VIS as well as NIR emission), the optically active species are present in more than one lattice configuration, where different ligand situations result in different relaxation times. The best fit of the experimental data was obtained with a double exponential equation,

$$I(t) = A + B_1 \cdot \exp\left(-t/\tau_1\right) + B_2 \cdot \exp(-t/\tau_2), \qquad (3)$$

where $I(t)$ is the emission intensity as a function of decay time t, $\tau_{1,2}$ are the characteristic lifetimes of two decay processes, and A, $B_{1,2}$ are fit parameters.

Values of 2.6 and 10.6 µs are obtained for $\tau_{1,2}$, respectively, of the Bi^{2+}-related VIS luminescence (Fig. 5(a)). This corresponds-well to common expectations, where the lifetime

#172414 - $15.00 USD Received 11 Jul 2012; revised 13 Aug 2012; accepted 14 Aug 2012; published 31 Aug 2012

of Bi^{2+}-related luminescence hardly exceeds 20 µs. For example, a value of ~10.5 µs has been reported for Bi^{2+} ions in crystalline $Bi_{12}GeO_{20}$ [39], ~11-13 µs in crystalline strontium borate [9], or ~20-25 µs in crystalline alkaline earth phosphates [7]. For NIR emission, the lifetime measurement yields values of 6.8 and 27.4 µs for $\tau_{1,2}$, respectively. Assumedly as a result of Bi-Bi interaction, these values are significantly lower than those which were previously reported for bismuth-doped alumina germanate glasses with low bismuth concentration [22], but are comparable to reports for bismuth cluster species [11].

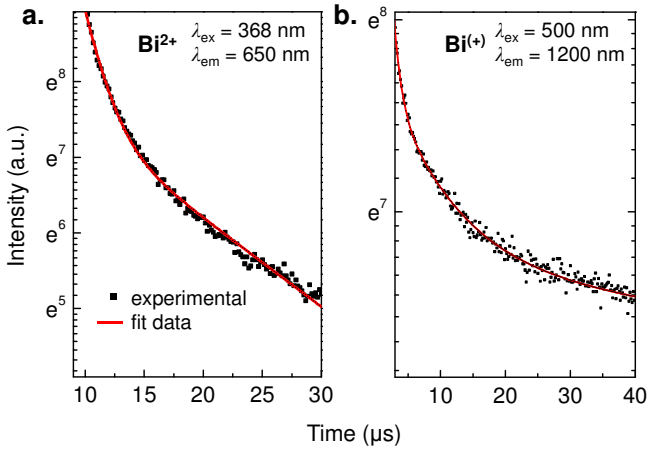

Fig. 5. Exemplary decay spectra of the $70.5GeO_2$ – $24.5Bi_2O_3$ – $5WO_3$. The solid line represents the best fit of the data to a double exponential function, Eq. (2).

4. Conclusions

Luminescence from cerium-doped $70.5GeO_2$ – $24.5Bi_2O_3$- $5WO_3$ glasses occurs from Bi^{2+} (VIS) and lower valence states (NIR). The intensity of both emission bands can be controlled via the amount of CeO_2, where the latter acts as an oxidant for the transformation of bismuth in lower valence states to Bi^{3+}. The parallel formation of Ce^{3+} leads to a trade-off in optical transparency in the visible spectral range. Optimal VIS transparency is obtained for a nominal CeO_2 concentration of x ~0.1-0.2 mol%. Ultrabroad NIR photoemission is erased at $x > 0.1$ mol%. Compared to lead germanate glasses, the intoxicity of bismuth(III)oxide provides a significant advantage for glass processing and application in optical devices. Using CeO_2 as an oxidant prevents formation of strongly coloring bismuth species. At appropriate composition and redox conditions, ultrabroad NIR luminescence from bismuth centers can be obtained without further dopants, but could be modified by the addition of co-dopants. This provides interest for optical amplifiers and lasers.

Acknowledgments

We acknowledge the German Academic Exchange Service (DAAD) and the Group of Eight (Go8) universities for funding this work under the DAAD-Go8 Germany-Australia joint research co-operation scheme. S.M. and H.E.-H. acknowledge the DSTO (Australia) for support for the Centre of Expertise in Photonics, and the Asian Office of Aerospace R&D (AOARD 104120) for funding this project. We wish to thank Rachel Moore at Adelaide University for her help with glass fabrication.